

Electronic Structure and Kinetics Calculations for the Si+SH Reaction, a Possible Route of SiS Formation in Star-Forming Regions

Marzio Rosi[1,2(✉)], Dimitrios Skouteris[3,4], Nadia Balucani[5,6,7], Luca Mancini[5], Noelia Faginas Lago[5], Linda Podio[6], Claudio Codella[6], Bertrand Lefloch[7], and Cecilia Ceccarelli[7]

[1] Dipartimento di Ingegneria Civile e Ambientale, Università degli Studi di Perugia, 06125 Perugia, Italy
marzio.rosi@unipg.it
[2] CNR-ISTM, 06123 Perugia, Italy
[3] Scuola Normale Superiore, 56126 Pisa, Italy
dimitrios.skouteris@sns.it
[4] Master-Up, Strada Vicinale Sperandio 15, 06125 Perugia, Italy
d.skouteris@master-up.it
[5] Dipartimento di Chimica, Biologia e Biotecnologie, Università degli Studi di Perugia, 06123 Perugia, Italy
{nadia.balucani,noelia.faginaslago}@unipg.it, mancinilucaOO@gmail.com
[6] INAF, Osservatorio Astrofisico di Arcetri, 50125 Florence, Italy
{lpodio,codella}@arcetri.inaf.it
[7] Université Grenoble Alpes, IPAG, 38000 Grenoble, France
{bertrand.lefloch,cecilia.ceccarelli}@univ-grenoble-alpes.fr

Abstract. The reaction between atomic silicon and the mercapto radical has been computationally investigated by means of electronic structure and kinetics calculations to establish its possible role in the formation of interstellar SiS. According to our kinetics estimates based on the electronic structure calculations of the Si+SH potential energy surface, the reaction is very fast reaching the gas-kinetics limit. Therefore, the title reaction is an efficient formation route of interstellar SiS provided that silicon atoms and mercapto radicals are present. Implications for the observation of an anomalously high abundance of SiS in the shocked region around a Sun-like protostar (L1157-B1) are also presented.

Keywords: Electronic structure calculations · Kinetics calculations · Astrochemistry · Silicon chemistry

1 Introduction

Since its first detection in 1975 by Morris et al. [1] towards the molecular envelope of the carbon-rich AGB star IRC+ 10216, silicon monosulfide (SiS) has been the object of sporadic detections, mostly in circumstellar envelopes around evolved stars [2, 3]. In

© Springer Nature Switzerland AG 2019
S. Misra et al. (Eds.): ICCSA 2019, LNCS 11621, pp. 306–315, 2019.
https://doi.org/10.1007/978-3-030-24302-9_22

addition to that, SiS detection has been achieved towards high mass star-forming regions with shocks (such as Sgr B2 and Orion KL [4–8]) and, more recently, in a shocked region, L1157-B1, around a low mass protostar [9]. The elements silicon and sulfur are relatively abundant in the universe with an atomic fraction of 30 and 16 ppm, respectively, and several species holding either a Si or an S atom have been detected so far [10]. Both Si and S are also expected to be depleted from the gas-phase on interstellar dust grains. For instance, most of interstellar silicon is retained in the silicates of interstellar dust particles and can only return to the gas phase after violent events, such as high intensity shocks that are able to sputter the refractory core of dust grains and release gaseous silicon. The most abundant interstellar silicon compound in the gas-phase is SiO, while SiS is much less abundant. In the case of L1157-B1, a shocked region driven by a fast jet ejected from a Sun-like protostar, a surprisingly high abundance of SiS has been observed in a delimited region around the protostar [9]. In that specific region, the relative abundance of SiS with respect to SiO is of the order of 0.04, that is much higher than the typical values (*ca.* 5×10^{-3}) for regions where SiS has been observed. The reasons for such a peculiar ratio remains a mistery and only a thourough comprehension of both silicon and sulphur interstellar chemistry can help us to understand the cause of this anomaly.

Until recently, very little was known about the SiS formation mechanisms. In an attempt to explain the L1157-B1 anomaly, recent theoretical work has been devoted to characterize the combined silicon/sulphur chemistry [11–13]. For instance, some of the present authors have characterized the potential energy surface of the reactions SiH+S and SiH+S_2 [11]. In addition, for the reaction H+SiS_2 we have performed kinetics calculations based on the capture theory and Rice-Ramsperger-Kassel-Marcus calculations [12]. In addition, Zanchet et al. [13] have suggested that the reactions Si+SO and Si+SO_2 can be responsible for SiS formation in the ouflows of star-forming regions like Sgr B2, Orion KL, and L1157-B1.

In this contribution we add another piece to the puzzle by reporting on a theoretical characterization of the potential energy surface (PES) and kinetics properties of the reaction Si+SH. As already mentioned, atomic silicon can be formed by the sputtering of the refractory silicates core in shocked regions like those of interest here. In addition, H_2S (the parent species of the SH radical) has been observed in L1157-B1 [14]. H_2S is easily converted into the SH radicals by chemical reactions or photodissociation [15]. In other words, Si and HS are plausible precursors of SiS if we can prove that the title reaction is efficient.

2 Computational Details

The Potential Energy Surface (PES) of the Si+SH was calculated employing a computational strategy which has been utilized with success in the past [16–19]. In this scheme the lowest stationary points, minima and transistion states, were optimized at the B3LYP level [20, 21] in conjunction with the aug-cc-pVTZ basis set [22, 23], augmented for S and Si with a tight d finction [24]. This basis set will be denoted aug-cc-pV(T + *d*)Z. At the same level of theory we have computed the harmonic vibrational frequencies in order to check the nature of the stationary points, i.e. minimum if

all the frequencies are real, saddle point if there is one, and only one, imaginary frequency. The assignment of the saddle points was performed using intrinsic reaction coordinate (IRC) calculations [25, 26]. The energy of the main stationary points was computed also at the more accurate coupled cluster theory with the inclusion of single and double excitations and a perturbative estimate of connected triples (CCSD(T)) [27–29] using the same basis set aug-cc-pV(T + *d*)Z. Both the B3LYP and the CCSD(T) energies were corrected to 0 K by adding the zero point energy correction; therefore all the energetic values are enthalpies at 0 K. The accuracy of the employed approach, in particular as far as basis set completeness is concerned, has been recently investigated [30]. For comparison purposes since the systems investigated are relatively small, we reoptimized the geometry of all the stationary points also at the CCSD(T)/aug-cc-pV(T + *d*)Z level. All calculations were performed using Gaussian 09 [31], while the analysis of the geometries and the vibrational frequencies was performed using Molekel [32, 33]. It is assumed that the reaction takes place on the ground electronic state but, otherwise, all possible paths have been taken into account.

Having determined the characteristics of the stationary points, we have performed kinetics calculations on the calculated PES, as done in previous work by some of the present authors for similar reactive systems [12, 16, 34–37]. Initially, the capture (Langevin) model is used to calculate the rate coefficient for the initial association of Si and SH. The long-range interaction potential (determined as a series of points through quantum calculations) was fitted to a $V(r) = -C/r^6$ equation (the typical interaction equation for two neutral species). Having obtained an association rate constant, we have calculated the corresponding dissociation rate coefficient through the detailed balance principle

$$k_{diss}(E) = k_{ass}(E) \times \rho_{reac}(E)/\rho_{comp}(E)$$

where $k_{ass}(E)$ is the association rate coefficient (as a function of energy), $\rho_{reac}(E)$ is the density of states per unit volume of the associating reactants at energy E and $\rho_{comp}(E)$ is the density of states of the initial complex at energy E. Through this scheme, we have seen that the dissociation rate coefficient is essentially negligible (the large depth of the potential energy well raises the density of states of the complex). From this, we can deduce that the initial association rate coefficient equals the sum of all rate coefficients leading to specific products, i.e. the total reaction rate constant.

The microcanonical reaction rate coefficient for each subsequent unimolecular step is calculated using the Rice-Ramsperger-Kassel-Marcus (RRKM) scheme (see, for instance, [38–42], whereby the rate coefficient is given by the expression

$$k(E) = \frac{N(E)}{h\rho(E)}$$

where *N(E)* is the number of microstates available in the transition state, *ρ(E)* is the density of states per unit volume of the reactants and *h* is Planck's constant. Subsequently, the rate constants are Boltzmann averaged to yield temperature-dependent ones. Tunnelling is taken account of by simulating each transition state by an Eckart barrier of the same energy and imaginary frequency.

3 Results

According to the present electronic structure calculations, the addition of the Si atom to the SH radical is a favored, barrierless process leading to the formation of a bound Si-S-H intermediate. The situation is rather similar to that observed in the isovalent reactions Si+OH [43, 44]. The optimized geometries of the stationary points located in the PES of the system Si+SH are reported in Fig. 1, while the energetics of the main processes involved in the Si+SH reaction is shown in Table 1. A schematic representation of the PES of the system Si+SH is presented in Fig. 2, where we have reported also the relative energies computed at B3LYP/aug-cc-pV(T + *d*)Z level and CCSD(T)/aug-cc-pV(T + *d*)Z level (in parentheses) at the B3LYP/aug-cc-pV(T + *d*)Z optimized geometries. When an Si atom approaches a SH radical, there is formation of a SiSH species in a very exothermic process, without any entrance barrier. SiSH, overcoming an energy barrier of almost 15 kcal/mol, can isomerize to the slightly more stable SSiH species or can dissociate into SiS+H, with a barrier which is very close to the endothermicity of the process. This is not surprising since this transition state is very late, showing an S—H distance very long (2.557 Å, see Fig. 1). SSiH can dissociate into SiS+H or S+SiH. Both reactions are endothermic, with an exit energy barrier which is equal to the endothermicity. The products S+SiH, moreover, lie above the reactants. From Fig. 2 and Table 1, we can see that the relative energies computed at B3LYP and CCSD(T) level (with the same geometries) differ by less than 3 kcal/mol. This is an expected result due to the different accuracy of the two methods. Since the investigated systems are relatively small, however, we decided to optimize the geometry of all the stationary points at CCSD(T)/aug-cc-pV(T + *d*)Z level.

Table 1. Enthalpy changes (kcal/mol, 0 K) computed at the B3LYP/aug-cc-pV(T + *d*)Z and CCSD(T)/aug-cc-pV(T + *d*)Z levels of theory for selected steps in the Si+SH reaction. Values in parentheses are computed at the optimized CCSD(T) geometries.

	ΔH_0^0		Barrier height	
	B3LYP	CCSD(T)	B3LYP	CCSD(T)
Si (^{3}P) + S (^{3}P) → SiS (($^1\Sigma^+$)	−139.2	−138.6 (−138.7)		
Si (^{3}P) + SH ($^2\Pi$) → SiSH	−83.2	−81.8 (−81.7)		
SiSH → SiS(($^1\Sigma^+$) + H (^{2}S)	26.8	24.8 (24.7)	27.0	25.7 (27.0)
SiSH → SSiH	−5.0	−3.6 (−3.7)	14.4	14.9 (14.9)
SSiH → SiS ($^1\Sigma^+$) + H (^{2}S)	31.8	28.4 (28.4)		
SSiH → S (^{3}P) + SiH ($^2\Pi$)	100.7	97.7 (97.7)		

From Fig. 1 we can notice that there is a very good agreement between the B3LYP and CCSD(T) geometries, with the only exception of the S—H distance in the transition state of the dissociation reaction of SiSH into SiS+H. From Fig. 3, where we have reported the relative energies computed at CCSD(T)/aug-cc-pV(T + *d*)Z level at the geometries optimized at the same level, we can notice that the barrier height for the reaction SiSH → SiS + H is slightly higher than before, confirming that B3LYP sometimes tends to underestimate energy barriers.

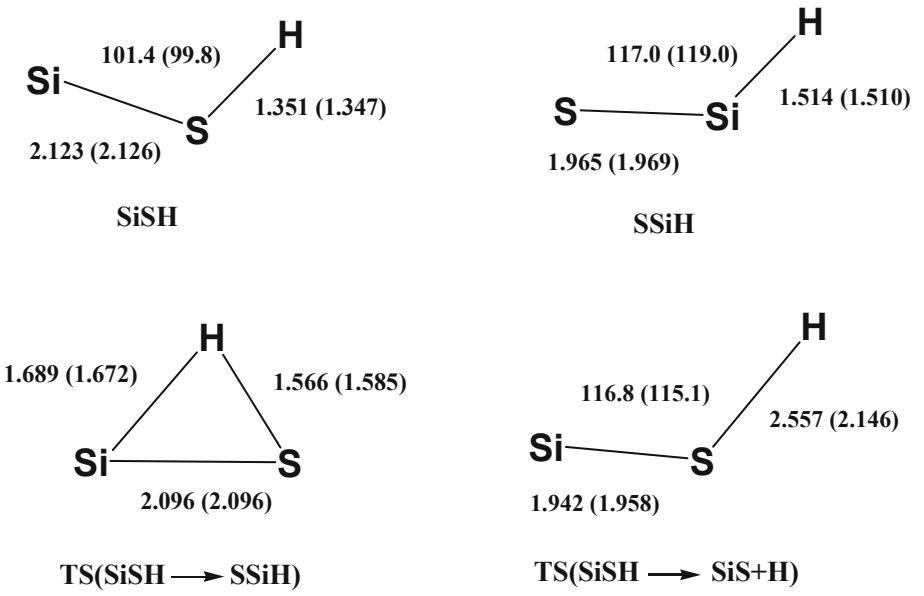

Fig. 1. B3LYP/aug-cc-pV(T + *d*)Z optimized geometries (Å and °) of minima and transition states for the SiSH system. Values in parentheses are optimized at CCSD(T)/aug-cc-pV(T + *d*)Z level.

The calculated rate coefficient as a function of temperature is shown in Fig. 4. As well visible, the rate coefficient is very high for the whole temperature range explored (from 0 to 500 K). The numerical value increases from 5.3×10^{-10} at 10 K to 8.6×10^{-10} at 100 K (a temperature typical of shocked regions) reaching a plateau at 300 K of ca. 1.0×10^{-9} cm^3 s^{-1}. The trend of the rate constant with temperature follows the capture rate constants calculated using a Langevin-like model. In particular, the capture rate constant, as a function of energy, reaches a plateau at high energies and this is reflected in the canonical rate constant after Boltzmann averaging.

The two factors that influence the value of the rate constant are the long-range attractive potential of the two reactant molecules and their reduced mass. The long-range potential tail has been fitted to an appropriate inverse power law and it has been found to be singularly high in this case. Moreover, the relatively high reduced mass of the reactants (roughly equal to the mass of the silicon atom) further contributes to enhance the corresponding cross section and rate coefficient.

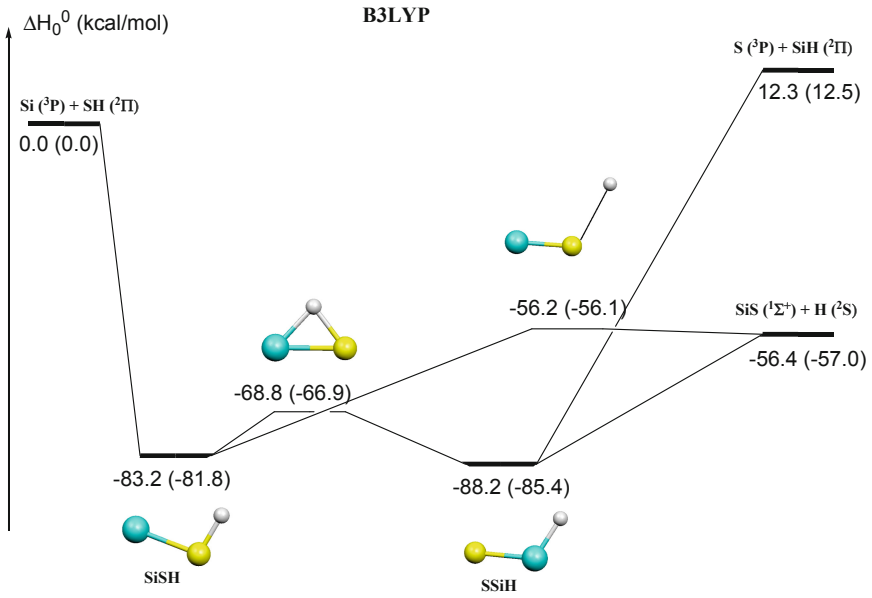

Fig. 2. Schematic representation of the Si+SH PES computed at B3LYP/aug-cc-pV(T + *d*)Z. Values in parentheses are CCSD(T)/aug-cc-pV(T + *d*)Z energies computed at the B3LYP optimized geometries.

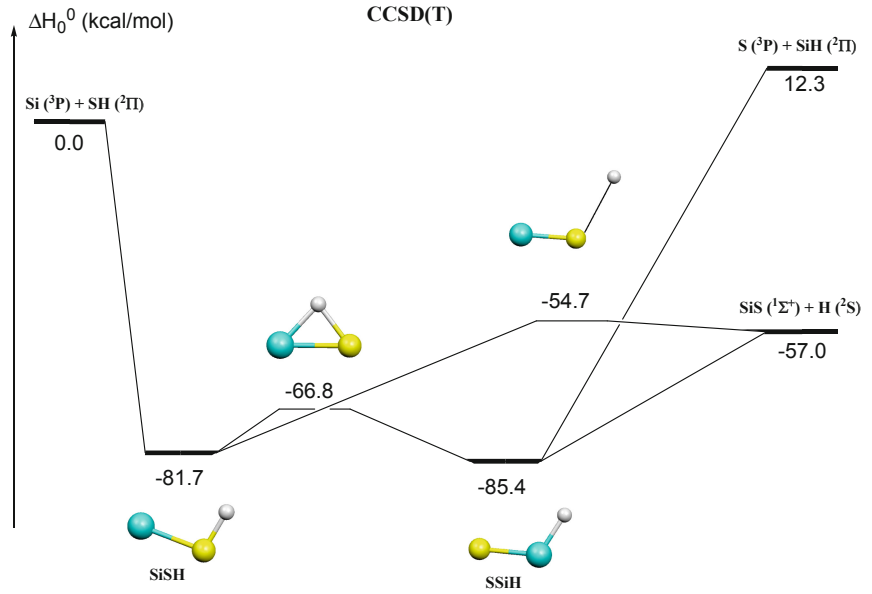

Fig. 3. Schematic representation of the Si+SH PES computed at CCSD(T)/aug-cc-pV(T + *d*)Z level.

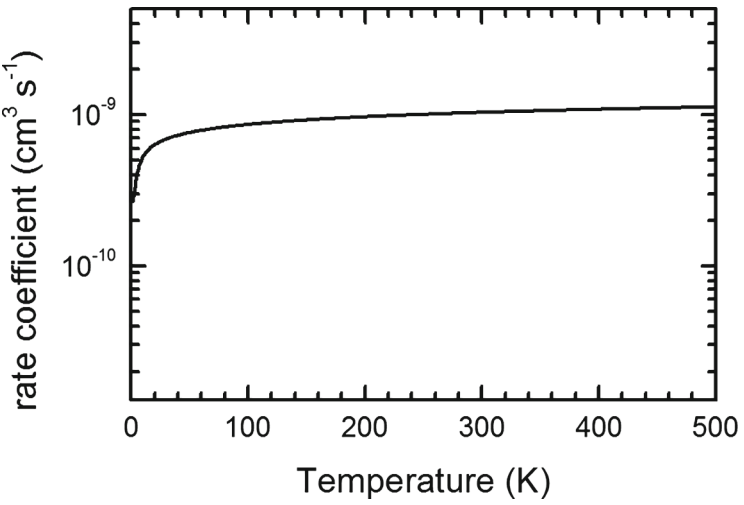

Fig. 4. Rate coefficients as a function of temperature for the title reaction (see text for details).

4 Implications for the Chemistry of Interstellar Silicon

As anticipated in the Introduction, the theoretical investigation on the reaction Si+SH reported here belongs to a systematic study that we have undertaken to understand the chemistry of interstellar silicon and, more specifically, to characterize the possible formation routes of SiS in low-mass star forming regions in gas-phase processes. This effort is necessary because the ion-molecule reactions invoked in previous models [45, 46] are not efficient, as proved by laboratory experiments (see [10] and references therein). In our first work on this subject, by performing electronic structure and kinetics calculations of the same kind reported here we have demonstrated that two bimolecular reactions involving the SiH radical and simple form of elemental sulphur (atomic sulphur, S, and disulphur, S_2) are viable routes of SiS formation [11]. The SiH radical is produced by silane photodissociation or by other high energy processes involving silane [47]. Indeed, recent work demonstrated that elemental silicon is preferentially converted into SiO or SiH_4 in the icy mantles of interstellar grains [48]. Atomic sulphur and disulphur are also relatively abundant and, therefore, their reactions could account for the observed amount of SiS. In a second paper, we have also investigated the reaction of H atoms (very abundant in the interstellar medium) with SiS_2 [12]. With that study, we have demonstrated that SiS_2 cannot be considered a stable reservoir of silicon because it is rapidly converted by H atoms into SiS. Therefore, every process that leads to SiS_2 is actually a step toward SiS formation. Finally, in this contribution we have demonstrated that the reaction between atomic silicon (possibly produced by the shock on silicate grains) and the mercapto radical SH (easily produced by its parent species H_2S already detected in L1157-B1 [14]) is also very fast, with rate coefficients reaching the gas kinetics limit.

We plan to use the derived rate coefficients in astrochemical models, as recently done for other cases [34–36, 49–51], to verify whether these processes are at work in

the ISM and can account for the observed overabundance of SiS in L1157-B1. Since silicon chemistry is mainly associated with shocked regions where elemental silicon is liberated in the gas phase, if we demonstrate that SiS is totally formed by neutral-neutral gas phase reactions, its presence and distribution in interstellar objects could become a kind of signpost for that type of chemistry being dominant in the above mentioned regions.

Acknowledgments. This work has been supported by MIUR "PRIN 2015" funds, project "STARS in the CAOS (Simulation Tools for Astrochemical Reactivity and Spectroscopy in the Cyberinfrastructure for Astrochemical Organic Species)", Grant Number 2015F59J3R and by the project PRIN-INAF 2016 The Cradle of Life - GENESIS-SKA (General Conditions in Early Planetary Systems for the rise of life with SKA). This project has received funding from the European Research Council (ERC) under the European Union's Horizon 2020 research and innovation programme, for the Project "The Dawn of Organic Chemistry" (DOC), grant agreement No 741002.

References

1. Morris, M., Gilmore, W., Palmer, P., Turner, B.E., Zuckerman, B.: Detection of interstellar SiS and a study of IRC+ 10216 molecular envelope. Astrophys. J. **199**, L47–L51 (1975)
2. Cernicharo, J., Guélin, M., Kahane, C.: A λ2 mm molecular line survey of the C-star envelope IRC+ 10216. Astron. Astrophys., Suppl. Ser. **142**, 181 (2000)
3. Prieto, L.V., et al.: Si-bearing molecules toward IRC+ 10216: ALMA unveils the molecular envelope of CWLeo. Astrophys. J. **805**, L13 (2015)
4. Dickinson, D.F., Kuiper, E.N.R.: Interstellar silicon sulfide. Astrophys. J. **247**, 112 (1981)
5. Ziurys, L.M.: SiS in Orion KL – Evidence for outflow chemistry. Astrophys. J. **324**, 544–552 (1988)
6. Ziurys, L.M.: SiS in outflow regions – more high-temperature silicon chemistry. Astrophys. J. **379**, 260–266 (1991)
7. Tercero, B., Vincent, L., Cernicharo, J., Viti, S., Marcelino, N.: A line-confusion limited millimeter survey of Orion KL II. Silicon-bearing species. Astron. Astrophys. **528**, A26 (2011)
8. MacKay, D.D.S.: The chemistry of silicon in hot molecular cores. Mon. Not. R. Astron. Soc. **274**, 694–700 (1995)
9. Podio, L., et al.: Silicon-bearing molecules in the shock L1157-B1: first detection of SiS around a Sun-like protostar. Mon. Not. R. Astron. Soc. Lett. **470**(1), L16–L20 (2017)
10. McGuire, B.A.: 2018 census of interstellar, circumstellar, extragalactic, protoplanetary disk, and exoplanetary molecules. Astrophys. J. Suppl. Ser. **239**, 17 (2018)
11. Rosi, M., et al.: Possible scenarios for SiS formation in the interstellar medium: electronic structure calculations of the potential energy surfaces for the reactions of the SiH radical with atomic sulphur and S_2. Chem. Phys. Lett. **695**, 87–93 (2018)
12. Skouteris, D., et al.: A theoretical investigation of the reaction H + $SiS_2$and implications for the chemistry of silicon in the interstellar medium. In: Gervasi, O., et al. (eds.) ICCSA 2018. LNCS, vol. 10961, pp. 719–729. Springer, Cham (2018). https://doi.org/10.1007/978-3-319-95165-2_50
13. Zanchet, A., Roncero, O., Agúndez, M., Cernicharo, J.: Formation and destruction of SiS in space. Astrophys. J. **862**, 38 (2018)

14. Holdship, K., et al.: H2S in the L1157-B1 bow shock. Mon. Not. R. Astron. Soc. **463**, 802 (2016)
15. Neufeld, D.A., et al.: Discovery of interstellar mercapto radicals (SH) with the GREAT instrument on SOFIA. Astron. Astrophys. **542**, L6 (2012)
16. Skouteris, D., Balucani, N., Faginas-Lago, N., Falcinelli, S., Rosi, M.: Dimerization of methanimine and its charged species in the atmosphere of Titan and interstellar/cometary ice analogs. Astron. Astrophys. **584**, A76 (2015)
17. Leonori, F., et al.: Crossed-beam and theoretical studies of the $S(^1D) + C_2H_2$ Reaction. J. Phys. Chem. A **113**, 4330–4339 (2009)
18. Troiani, A., Rosi, M., Garzoli, S., Salvitti, C., de Petris, G.: Vanadium hydroxide cluster ions in the gas phase: bond-forming reactions of doubly-charged negative ions by SO_2-promoted V-O activation. Chem. Eur. J. **23**, 11752–11756 (2017)
19. Berteloite, C., et al.: Low temperature kinetics, crossed beam dynamics and theoretical studies of the reaction $S(^1D) + CH_4$ and low temperature kinetics of $S(^1D) + C_2H_2$. Phys. Chem. Chem. Phys. **13**, 8485 (2011)
20. Becke, A.D.: Density functional thermochemistry. III. The role of exact exchange. J. Chem. Phys. **98**, 5648–5652 (1993)
21. Stephens, P.J., Devlin, F.J., Chablowski, C.F., Frisch, M.J.: Ab initio calculation of vibrational absorption and circular dichroism spectra using density functional force fields. J. Phys. Chem. **98**, 11623–11627 (1994)
22. Dunning Jr., T.H.: Gaussian basis sets for use in correlated molecular calculations. I. The atoms boron through neon and hydrogen. J. Chem. Phys. **90**, 1007–1023 (1989)
23. Woon, D.E., Dunning Jr., T.H.: Gaussian basis sets for use in correlated molecular calculations. III. The atoms aluminum through argon. J. Chem. Phys. **98**, 1358–1371 (1983)
24. Dunning Jr., T.H., Peterson, K.A., Wilson, A.K.: Gaussian basis sets for use in correlated molecular calculations. X. The atoms aluminum through argon revisited. J. Chem. Phys. **114**, 9244–9253 (2001)
25. Gonzalez, C., Schlegel, H.B.: An improved algorithm for reaction path following. J. Chem. Phys. **90**, 2154–2161 (1989)
26. Gonzalez, C., Schlegel, H.B.: Reaction path following in mass-weighted internal coordinates. J. Phys. Chem. **94**, 5523–5527 (1990)
27. Bartlett, R.J.: Many-body perturbation theory and coupled cluster theory for electron correlation in molecules. Annu. Rev. Phys. Chem. **32**, 359–401 (1981)
28. Raghavachari, K., Trucks, G.W., Pople, J.A., Head-Gordon, M.: Quadratic configuration interaction. A general technique for determining electron correlation energies. Chem. Phys. Lett. **157**, 479–483 (1989)
29. Olsen, J., Jorgensen, P., Koch, H., Balkova, A., Bartlett, R.J.: Full configuration–interaction and state of the art correlation calculations on water in a valence double-zeta basis with polarization functions. J. Chem. Phys. **104**, 8007–8015 (1996)
30. Rosi, M., et al.: An experimental and theoretical investigation of 1-butanol pyrolysis. Front. Chem. **7**, 326 (2019). https://doi.org/10.3389/fchem.2019.00326
31. Frisch, M.J., et al.: Gaussian 09, Revision A. 02. Gaussian, Inc., Wallingford (2009)
32. Flükiger, P., Lüthi, H.P., Portmann, S., Weber, J.: MOLEKEL 4.3. Swiss Center for Scientific Computing, Manno (2000–2002)
33. Portmann, S., Lüthi, H.P.: MOLEKEL: an interactive molecular graphics tool. Chimia **54**, 766–769 (2000)
34. Barone, V., et al.: Gas-phase formation of the prebiotic molecule formamide: insights from new quantum computations. Mon. Not. R. Astron. Soc. Lett. **453**, L31–L35 (2015)

35. Skouteris, D., Vazart, F., Ceccarelli, C., Balucani, N., Puzzarini, C., Barone, V.: New quantum chemical computations of formamide deuteration support gas-phase formation of this prebiotic molecule. Mon. Not. R. Astron. Soc. Lett. **468**, L1–L5 (2017)
36. Skouteris, D., et al.: The genealogical tree of ethanol: gas-phase formation of glycolaldehyde, acetic acid and formic acid. Astrophys. J. **854**, 135 (2018)
37. Vazart, F., Latouche, C., Skouteris, D., Balucani, N., Barone, V.: Cyanomethanimine isomers in cold interstellar clouds: insights from electronic structure and kinetic calculations. Astrophys. J. **810**, 111 (2015)
38. Leonori, F., et al.: Crossed-beam dynamics, low-temperature kinetics, and theoretical studies of the reaction $S(^1D) + C_2H_4$. J. Phys. Chem. A **113**, 15328–15345 (2009)
39. Balucani, N., et al.: Combined crossed beam and theoretical studies of the $N(^2D) + C_2H_4$ reaction and implications for atmospheric models of Titan. J. Phys. Chem. A **116**, 10467–10479 (2012)
40. Leonori, F., Skouteris, D., Petrucci, R., Casavecchia, P., Rosi, M., Balucani, N.: Combined crossed beam and theoretical studies of the $C(^1D) + CH_4$ reaction. J. Chem. Phys. **138**(2), 024311 (2013)
41. Balucani, N., et al.: Formation of nitriles and imines in the atmosphere of Titan: combined crossed-beam and theoretical studies on the reaction dynamics of excited nitrogen atoms $N(^2D)$ with ethane. Faraday Discuss. **147**, 189–216 (2010)
42. Balucani, N., et al.: Combined crossed molecular beam and theoretical studies of the $N(^2D) + CH_4$ reaction and implications for atmospheric models of Titan. J. Phys. Chem. A **113**, 11138–11152 (2009)
43. Dayou, D., Duflot, D., Rivero-Santamaría, A., Monnerville, M.: A global ab initio potential energy surface for the X^2A' ground state of the Si + OH → SiO + H reaction. J. Chem. Phys. **139**, 204305 (2013)
44. Rivero-Santamaría, A., Dayou, D., Rubayo-Soneirac, J., Monnerville, M.: Quasi-classical trajectory calculations of cross sections and rateconstants for the Si + OH → SiO + H reaction. Chem. Phys. Lett. **610–611**, 335–340 (2014)
45. Wakelam, V., et al.: The 2014 KIDA network for interstellar chemistry. Astrophys. J. Suppl. Ser. **217**(2), 20 (2015)
46. McElroy, D., Walsh, C., Markwick, A.J., Cordiner, M.A., Smith, K., Millar, T.J.: The UMIST database for astrochemistry 2012. Astron. Astrophys. **550**, A36 (2013)
47. Yang, T., Thomas, A.M., Dangi, B.B., Kaiser, R.I., Mebel, A.M., Millar, T.J.: Directed gas phase formation of silicon dioxide and implications for the formation of interstellar silicates. Nat. Commun. **9**, 774 (2018)
48. Ceccarelli, C., Viti, S., Balucani, N., Taquet, V.: The evolution of grain mantles and silicate dust growth at high redshift. Mon. Not. R. Astron. Soc. **476**, 1371–1383 (2018)
49. Balucani, N., Ceccarelli, C., Taquet, V.: Formation of complex organic molecules in cold objects: the role of gas-phase reactions. Mon. Not. R. Astron. Soc. **449**, L16–L20 (2015)
50. Skouteris, D., et al.: Interstellar dimethyl ether gas-phase formation: a quantum chemistry and kinetics study. Mon. Not. R. Astron. Soc. **482**, 3567–3575 (2019)
51. Ascenzi, D., Cernuto, A., Balucani, N., Tosi, P., Ceccarelli, C., Martini, L. M., Pirani, F.: Destruction of dimethyl ether and methyl formate by collisions with He^+. Astronom. Astrophys. (2019, in press). https://doi.org/10.1051/0004-6361/201834585